

## Geometric and Energetic Aspects of Aluminum Nitride Cages

Hai-Shun Wu,<sup>\*,†</sup> Fu-Qiang Zhang,<sup>†</sup> Xiao-Hong Xu,<sup>†</sup> Cong-Jie Zhang,<sup>†</sup> and Haijun Jiao<sup>\*,†,‡</sup>*Department of Chemistry, Shanxi Normal University, Linfen, 041004, China, and Institut für Organische Katalyseforschung (IfOK) an der Universität Rostock e.V., Buchbinderstrasse 5–6, 18055 Rostock, Germany**Received: October 24, 2002*

The structure and energy of aluminum nitride cages  $(\text{AlN})_n$  ( $n = 2-41$ ) have been investigated theoretically. The most stable cages have been constructed on the basis of a simple design principle, and the predicated stability has been validated at the B3LYP/LANL2DZp//HF/LANL2DZ level of theory. Among these, the  $T_h$  symmetrical  $(\text{AlN})_{12}$  cluster has been computed to be the most stable cage on the basis of the calculated disproportionation energy and binding energy per AlN unit.

## Introduction

Aluminum nitride (AlN) ceramics, because of their excellent physical and chemical properties as high thermal-conductivity, low thermal-inflate coefficient, chemical inertness, and large energy gap, have attracted considerable attention to physics, chemistry, and material science.<sup>1</sup> These materials can be produced, for example, by chemical vapor deposition from aluminum salts reacting with ammonia<sup>2,3</sup> or from organometallic precursors.<sup>4</sup> Under vacuum condition and using magnetron reactive sputtering technique, the sputtered Al atoms can react with  $\text{N}_2$  to form a new-type AlN nanofilm, and some  $\text{Al}_n\text{N}_m$  precursor intermediates have been experimentally already observed.<sup>5</sup> AlN clusters can also be produced by nitrogen ion beam bombardment of aluminum target.<sup>6</sup> In addition,  $\text{Al}_x\text{N}_y$  species ( $x = 1-3$ ,  $y = 1-3$ ) have been produced by reactions of laser-ablated Al atoms with N atoms, and their possible structures were proposed on the basis of infrared spectra, compared with the results of density functional theory.<sup>7</sup> Using laser ionization time-of-flight mass spectroscopic method, Chu suggested that  $(\text{AlN})_{10}$  is likely to yield highly oriented crystalline thin films when deposited on a substrate.<sup>8</sup> More recently, several hexameric aluminum imides with an  $(\text{AlN})_6$  hexagonal drum unit bearing substituents have been synthesized and characterized by single-crystal structural analysis.<sup>9</sup>

Theoretically, the structure and bonding of  $\text{R}_2\text{Al}=\text{NH}_2$ , considered as a possible AlN precursor, have been investigated.<sup>10,11</sup> Matsunaga<sup>12</sup> carried out theoretical investigations on the structures of  $(\text{XAlNH})_3$  and found that the benzene-like structure is the most stable isomer, as compared to the prism, boat, and chair forms. Using the calculated thermodynamic stability of a set of  $\text{X}_m(\text{AlN})_n\text{H}_m$  clusters, Timoshkin<sup>13</sup> discussed the mechanism of  $(\text{AlN})_n$  cluster formations. On the basis of local density functional calculations, Grimes<sup>14</sup> analyzed the structure and bonding of  $(\text{AlN})_n$  ( $n = 1-4$ ) clusters and found that the cluster stability increases with the increased size. In agreement with the experimental findings,<sup>15</sup> all computations show that monomer  $(\text{AlN})_1$  has a triplet ground state and the singlet state is higher in energy,<sup>16</sup> and the high level ab initio (MRCI) and density functional (BP86) calculated dissociation energies, bond distances, and vibration frequencies are close to

the experimental values. Using density functional method, BelBruno<sup>17</sup> studied the structure and stability of a set of small  $(\text{AlN})_n$  ( $n = 2-4$ ) clusters and found that the most stable structures are  $D_{nh}$  symmetrical and that the eight-membered  $D_{4h}$  monocyclic ring structure of  $(\text{AlN})_4$  is more stable than the caged form. That the  $D_{3h}$  monocyclic  $(\text{AlN})_3$  is the most stable trimer<sup>17</sup> is confirmed by Pandey.<sup>18</sup>

On the basis of the computed structures and thermodynamics properties of  $(\text{AlN})_n$  ( $n = 1-15$ ),<sup>19</sup>  $(\text{HAlNH})_n$  ( $n = 1-15$ ),<sup>20</sup> and  $(\text{ClAlNH})_n$  ( $n = 1-15$ ),<sup>21</sup> Wu found that these clusters have similar stability order; that is, the stability of clusters with even-numbered  $n$  is higher than those with odd-numbered  $n$ . Recently, structures of energetically low-lying stationary states of small  $(\text{AlN})_n$  clusters ( $n = 1, 2, 4, 6$ , and  $12$ ) have been computed at the BP86 density functional level of theory, and it is found that cage-like species become more favorable than planar arrangements with increased cluster size and that  $(\text{AlN})_{12}$  cage has extraordinary stability.<sup>16</sup> In addition to AlN cages, related  $\text{Al}_x\text{N}_y$  clusters are also analyzed theoretically.<sup>22</sup> With the increased research intensity of AlN thin film materials and the discovery of new  $(\text{AlN})_n$  clusters, further extensive investigations on  $(\text{AlN})_n$  clusters are of experimental and theoretical importance.

Because all of the reported studies are concentrated on small clusters, we present our theoretical studies on the structure and stability of large sized  $(\text{AlN})_n$  ( $n = 2-41$ ) clusters. First, we discussed a mathematical design principle to consider the relationship between the four- and six-membered rings and then the relationship among symmetry and size, and stability of clusters. Finally, these qualitative results were validated on the basis of ab initio and density functional calculations and compared with those of the structural related  $(\text{BN})_n$  cages from density functional tight-binding results.<sup>23</sup>

## Computation Method

In this paper, designing molecular structure, determining symmetry, and adjusting input parameters were carried out using a program developed by ourselves.<sup>24</sup> For selecting the most stable isomers, all proposed structures were fully optimized first using the AM1 method.<sup>25</sup> The obtained most stable  $(\text{AlN})_n$  structures were further refined ( $n = 2-41$ ) and characterized as energy minima ( $n = 2-28$ , with only real frequencies, and the number of imaginary frequencies is zero,  $\text{NImag} = 0$ ) at the Hartree–Fock (HF) level with the LANL2DZ basis set (HF/LANL2DZ). The final energies were the single-point energies

\* To whom correspondence should be addressed. E-mail: hjiao@ifok.uni-rostock.de.

<sup>†</sup> Shanxi Normal University.

<sup>‡</sup> IfOK an der Universität Rostock e.V.

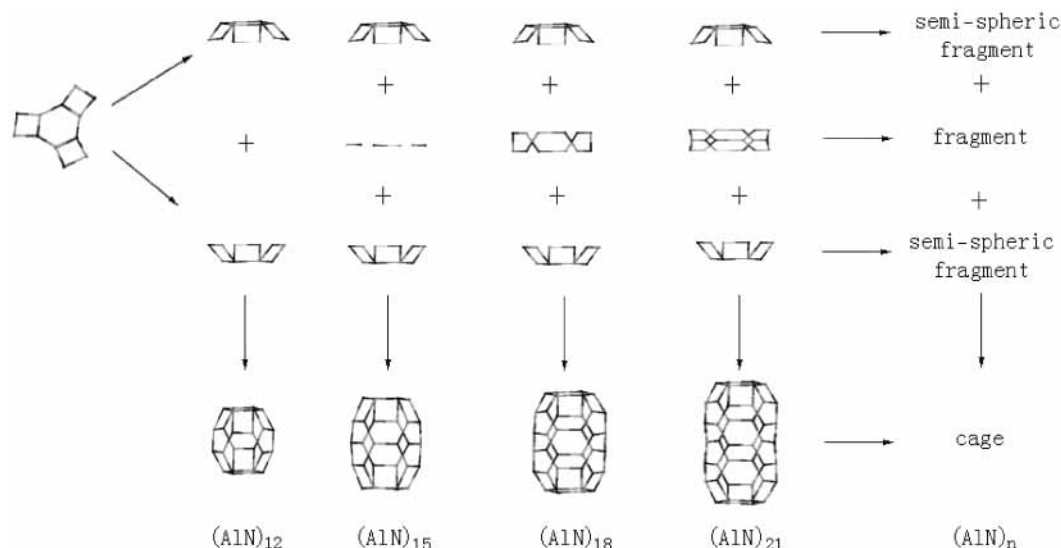


**Figure 1.**  $(\text{AlN})_n$  cluster formation from molecular fragments.

( $n = 2-31$ ) at the B3LYP level with the LANL2DZ basis set including an additional set of polarization function (LANL2DZp) on the HF/LANL2DZ geometries (B3LYP/LANL2DZp//LANL2DZ).<sup>26</sup> Some test calculations were carried out at the B3LYP level with the 6-31G\* and 6-311G\* basis sets. All calculations were done with the Gaussian 98 program.<sup>27</sup> The calculated total electronic energies, zero-point energies, and Cartesian coordinates are summarized in the Supporting Information.

## Results and Discussions

**Design Principle.** On the basis of the previous investigations on  $(\text{AlN})_n$  cages,<sup>21</sup> it is found that isomers without direct Al–Al and N–N bondings are more stable, and such a relation can only be observed in even-numbered (four, six, or eight) rings. To construct  $(\text{AlN})_n$  cages, it is necessary to gain some insight into the relationship between four- ( $f_4$ ), six- ( $f_6$ ), and eight-membered ( $f_8$ ) faces in polyhedrons. Indeed, such a relationship has been analyzed and discussed by Ziegler on the basis of the calculated structure and stability of 36 different methylaluminumoxane cages with the general formula  $(\text{MeAlO})_n$  ( $n = 14-16$ ).<sup>28</sup> It is found that cages containing  $f_4$  and  $f_8$  faces are less stable than those with  $f_4$  and  $f_6$ . For cages consisting of  $f_4$  and  $f_6$  faces, the number of  $f_4$  is always equal to 6 ( $f_4 = 6$ ), whereas the number of  $f_6$  is  $n - 4$  ( $f_6 = n - 4$ ), as deduced from the Euler polytope.<sup>29</sup> This mathematical relationship is true for any trivalent polyhedron containing only  $f_4$  and  $f_6$  faces. Thus, with the increased cluster size, the number of  $f_6$  increases, whereas that of  $f_4$  is constant. For example, both  $(\text{AlN})_7$  and  $(\text{AlN})_9$  have six  $f_4$ , whereas the former has three and the latter has five  $f_6$ , respectively. Furthermore, for large cages, the probability of an atom bonded to three  $f_4$  becomes very small, and the same is also true for an atom connecting to two  $f_4$  and one  $f_6$ .

**Design Method.** On the basis of the design principle discussed above, the stability of the constructed isomers of a  $(\text{AlN})_n$  cluster depends on the separation of the six  $f_4$  faces; that is, the larger the separation, the more stable the system, and the molecule with maximal separation of  $f_4$  should be the most stable structure, in line with the pentagon rule in fullerene chemistry.<sup>30</sup> Therefore, the number of stable isomers is rather limited, and one might also expect that large cages with well-separated  $f_4$  can have several isomers very close in energy, and the potential energy surfaces become shallow rather than deep.

For constructing cages, the best way is to start with the configuration having maximum distances among the six  $f_4$  and then to adjust their relative positions. Here, we analyze four  $(\text{AlN})_n$  ( $n = 12, 15, 18,$  and  $21$ ) cages as assembled two semispherical fragments with a cylinder tube as shown in Figure 1, and all the four clusters have the same fragment with different sizes of cylinder tubes. Thus, molecule design becomes docking of “semispherical fragments”. In addition, the size of fragments can be extended without changing symmetry, and large fragments with related cylinder tubes can form large-sized cages. From this point of view, the final symmetry of the constructed molecules was determined by the symmetry of the fragments and the relative positions of the six  $f_4$ .

For large clusters, we have constructed 16 fragments as shown in Figure 2. From the view of their shapes, they can have different symmetries, i.e.;  $C_4$  for 1–2,  $C_3$  for 3–8, and  $C_2$  for 9–16. The extended fragments 1’–16’ in the corresponding symmetries also are shown in Figure 2. Using the fragments in Figure 2, one can construct easily all possible cage isomers of  $(\text{AlN})_n$  ( $n \leq 41$ ).

**Symmetry.** For constructing small-sized cages, docking of “molecule fragments” is an effective and sufficient method. On this basis, we have constructed a set of  $(\text{AlN})_n$  ( $n = 2-41$ ) cluster isomers in lower energies. As shown in Figure 3, the relatively small-sized cages were annelated or connected by two small fragments, i.e.,  $(\text{AlN})_9/3 + 3$ ,  $(\text{AlN})_{10}/12' + 12'$ ,  $(\text{AlN})_{12}/1 + 1$ ,  $(\text{AlN})_{16}/1 + 1$ ,  $(\text{AlN})_{27}/5 + 5$ , and  $(\text{AlN})_{30}/12' + 12' + 1$ , respectively. The cluster symmetry is generally determined by the fragment symmetry and relative position, for example,  $(\text{AlN})_9$  has  $D_{3h}$  symmetry, whereas its fragment 3 is  $C_3$  symmetrical. This relationship has been confirmed by HF/LANL2DZ frequency calculations, and structures  $(\text{AlN})_n$  in the given symmetry ( $n = 2-28$ ) are found to be energy minima in the given symmetry without imaginary frequencies ( $\text{NImag} = 0$ ) as given in the Supporting Information.

Table 1 collects the relationship between symmetry and size of clusters. For small cages, the number of the more stable isomers is very limited. For example,  $(\text{AlN})_{16}$  can have four possible structures in  $T_d$ ,  $C_{3v}$ ,  $C_3$ , and  $S_4$  symmetry, and the most stable isomer may be  $T_d$  symmetrical with the maximum distances among the six  $f_4$ .

**Stability.** To validate these qualitative results, HF/LANL2DZ computations on the most stable AMI structures were carried

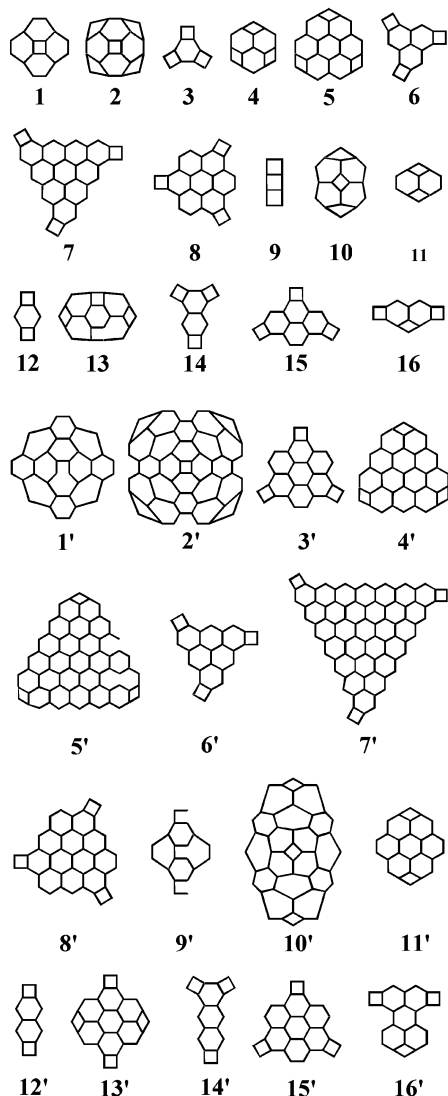


**Figure 2.** Configuration of molecular fragments 1–16 and 1'–16'.

out. At the HF/LANL2DZ level, the calculated relative energies, especially the most stable isomers, agree with the qualitative analysis on the basis of symmetry and design principle. For example, the most stable structure of  $(\text{AlN})_{16}$  has  $T_d$  symmetry, whereas the other isomers are higher in energy by 17.3/ $C_{3v}$ , 114.4/ $C_3$ , and 177.6/ $S_4$  kcal/mol at HF/LANL2DZ (0.0/ $T_d$ , 16.7/ $C_{3v}$ , 84.4/ $C_3$ , and 134.7/ $S_4$  kcal/mol at B3LYP/LANL2DZp//HF/LANL2DZ and 0.0/ $T_d$ , 11.0/ $C_{3v}$ , 80.9/ $C_3$ , and 125.4/ $S_4$  kcal/mol at B3LYP/cc-PVDZ).<sup>31</sup> The energy differences among the five most stable  $(\text{AlN})_{36}$  isomers are smaller than 7 kcal/mol (0.0/ $C_{3h}$ , 4.1/ $T_d$ , 5.8/ $C_3$ , 5.9/ $C_2$ , and 6.4/ $S_6$  kcal/mol) at HF/LANL2DZ. For the small monocyclic structures ( $n = 2, 4$ , and 6), the most stable forms in this paper agree well with the results at highly correlated levels of theory.<sup>16–18</sup>

The stability of the most stable  $(\text{AlN})_n$  clusters is tested by using the monomer binding energy ( $\Delta E_n$ ), as defined in eq 1, in which  $E_{\text{AlN}}$  is the energy of AlN monomer in the more stable triplet state (both HF/LANL2DZ and B3LYP/LANL2DZp favor the triplet state over the singlet state<sup>16</sup>) and  $E_n$  is the energy of the bulky cluster. The same method has been used to estimate the most stable isomer and the effect of cage size on the binding energy of  $(\text{BN})_n$  clusters<sup>23</sup> and  $(\text{MeAlO})_n$  cages.<sup>28</sup>

$$\Delta E_n = E_{\text{AlN}} - (1/n)E_n \quad (1)$$

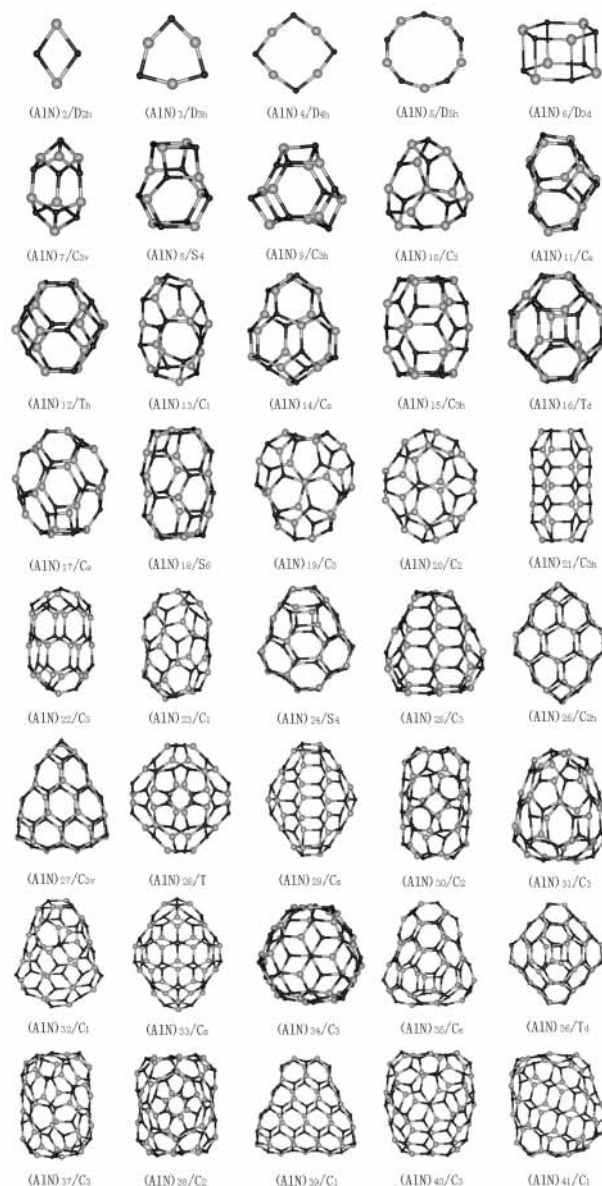


**Figure 3.** Most stable  $(\text{AlN})_n$  cages ( $n = 2-41$ ).

All these data are given in Table 2, and the binding energy of the most stable isomer as a function of cage size is shown in Figure 4. Both data calculated at HF/LANL2DZ and B3LYP/LANL2DZp//LANL2DZ show the same trend and pattern, although they differ quantitatively. With increased cluster size, one can see clearly that the difference between  $\Delta E_n$  and  $\Delta E_{n+1}$  decreases rapidly. This change is mainly attributed to the reduced angle strain with increased cage size as pointed out by Ziegler.<sup>28</sup> It is to note that monocyclic  $(\text{AlN})_n$  ( $n = 2-5$ ) have only bivalent bonds, whereas all other cluster are trivalent.

It is also easily and clearly seen that the binding energies per AlN of some clusters ( $n = 12$  and 16, Table 2) are larger than those of their neighbors, and the largest difference is found for  $(\text{AlN})_{12}$  by 5.9 and 3.0 kcal/mol at B3LYP/LANL2DZp//LANL2DZ (7.9 vs 4.1 kcal/mol at HF/LANL2DZ; 5.9 vs 3.2 kcal/mol at B3LYP/6-31G\*, and 5.9 vs 3.4 kcal/mol at B3LYP/6-311G\*//B3LYP/6-31G\*, respectively, indicating that larger basis set does change the relative energies), revealing the special stability. The same trend has been found for the structural related  $(\text{BN})_n$  clusters.<sup>23</sup>

For checking the relative stability of individual cages, we used  $\Delta^2 E_n$  from eq 2, where,  $E_{n+1}$ ,  $E_{n-1}$ , and  $E_n$  are the energies



TABLE 1: Relationship between Symmetry and Size of  $(\text{AlN})_n$  Cluster Isomers

symm	relation	$n$
$T_d$	$n = 4k^2$	$n = 4, 16, 36, 64, \dots$
$T_h$	$n = 12k^2$	$n = 12, 48, 108, \dots$
$T$	$n = 4(I + 6k)$	$n = 28, 52, 76, \dots$
$D_{3h}$	$n = 18k^2$	$n = 18, 72, \dots$
$D_{3d}$	$n = 6k^2$	$n = 6, 24, 54, \dots$
$C_{3h}$	$n = 3 + 6k, 12 + 12k$	$n = 9, 15, 21, 24, 27, 33, 36, 39, 45, 48, \dots$
$C_{3v}$	$n = 13 + 3k$	$n = 13, 16, 27, 30, 40, 45, 51, 54, \dots$
$S_6$	$n = 6 + 6k$	$n = 18, 24, 30, 36, 42, 48, 54, 60, \dots$
$C_3$	$n = 7 + 3k, 24 + 6k$	$n = 10, 16, 19, 22, 25, 27, 28, 30, 31, 34, 36, \dots$
$C_{2h}$	$n = 6 + 4k, 28 + 4k$	$n = 10, 14, 18, 22, 26, 30, 32, 34, 38, 40, 42, 44, \dots$
$C_{2v}$	$n = 12 + 12k$	$n = 24, 36, 48$
$S_4$	$n = 8 + 4k$	$n = 12, 16, 20, 24, 28, 32, 36, 40, 44, \dots$
$C_2$	$n = 18 + 2k$	$n = 18, 20, 22, 24, 28, 30, 32, 34, 36, 38, 42, 44, \dots$
$C_s$	$n = 9 + 3k, 15 + 3k, 19 + 6k$	$n = 11, 14, 17, 18, 21, 23, 24, 25, 26, 27, 29, 30, 31, 32, 33, 35, 37, 38, \dots$

TABLE 2: Energies (kcal/mol) of the Most Stable  $(\text{AlN})_n$  Cages

$(\text{AlN})_n/\text{sym}$	$\Delta E_n^a$	$\Delta^2 E_n^b$	$(\text{AlN})_n/\text{sym}$	$\Delta E_n^a$	$\Delta^2 E_n^b$
$(\text{AlN})_2/D_{2h}$	36.6 (79.4)	33.9 (38.5)	$(\text{AlN})_{22}/C_3$	113.4 (150.5)	10.0 (15.9)
$(\text{AlN})_3/D_{3h}$	26.1 (80.2)	-53.3 (-27.9)	$(\text{AlN})_{23}/C_1$	113.5 (150.1)	-11.1 (-17.4)
$(\text{AlN})_4/D_{4h}$	47.6 (94.5)	7.3 (7.2)	$(\text{AlN})_{24}/S_4$	114.5 (151.1)	-1.0 (-3.5)
$(\text{AlN})_5/D_{5h}$	57.5 (100.2)	-8.0 (-35.0)	$(\text{AlN})_{25}/C_3$	115.5 (152.4)	9.0 (14.5)
$(\text{AlN})_6/D_{3d}$	66.8 (115.7)	22.4 (38.8)	$(\text{AlN})_{26}/C_{2h}$	115.8 (152.4)	-6.2 (-11.5)
$(\text{AlN})_7/C_{3v}$	67.1 (115.7)	-50.9 (-39.6)	$(\text{AlN})_{27}/C_{3v}$	116.5 (153.3)	-9.5 (7.1)
$(\text{AlN})_8/S_4$	80.0 (125.6)	17.1 (12.8)	$(\text{AlN})_{28}/T$	117.8 (153.6)	21.8 (-2.1)
$(\text{AlN})_9/C_{3h}$	86.2 (130.4)	20.4 (16.5)	$(\text{AlN})_{29}/C_s$	117.5 (154.1)	-3.7 (1.5)
$(\text{AlN})_{10}/C_3$	87.2 (131.0)	-32.9 (-24.7)	$(\text{AlN})_{30}/C_2$	117.5 (154.4)	-21.2 (-10.1)
$(\text{AlN})_{11}/C_s$	93.9 (136.0)	-13.9 (-10.5)	$(\text{AlN})_{31}/C_3$	118.9 (155.3)	21.7
$(\text{AlN})_{12}/T_h$	101.8 (141.9)	70.4 (51.8)	$(\text{AlN})_{32}/C_1$	118.9	-7.5
$(\text{AlN})_{13}/C_1$	97.7 (138.9)	-54.2 (-39.9)	$(\text{AlN})_{33}/C_s$	119.2	-10.0
$(\text{AlN})_{14}/C_s$	101.9 (142.0)	-6.5 (-4.4)	$(\text{AlN})_{34}/C_3$	120.2	9.3
$(\text{AlN})_{15}/C_{3h}$	106.4 (145.3)	14.5 (8.9)	$(\text{AlN})_{35}/C_s$	120.6	-2.3
$(\text{AlN})_{16}/T_d$	108.5 (147.1)	26.8 (22.8)	$(\text{AlN})_{36}/T_d$	121.0	-2.8
$(\text{AlN})_{17}/C_s$	107.3 (146.0)	-31.5 (-24.2)	$(\text{AlN})_{37}/C_s$	121.6	10.6
$(\text{AlN})_{18}/S_6$	109.6 (147.7)	27.1 (17.9)	$(\text{AlN})_{38}/C_2$	121.7	-5.5
$(\text{AlN})_{19}/C_3$	108.9 (147.3)	-19.2 (-13.4)	$(\text{AlN})_{39}/C_1$	121.9	-2.6
$(\text{AlN})_{20}/C_2$	110.2 (148.3)	-10.0 (-3.2)	$(\text{AlN})_{40}/C_3$	122.3	0.0
$(\text{AlN})_{21}/C_{3h}$	112.3 (149.5)	9.1 (0.7)	$(\text{AlN})_{41}/C_1$	122.7	

<sup>a</sup> Binding energy from eq 1 at HF/LANL2DZ (the B3LYP/LANL2DZp//HF/LANL2DZ values are in parentheses). <sup>b</sup> Disproportionation energy from eq 2 at HF/LANL2DZ (the B3LYP/LANL2DZp values are in parentheses).

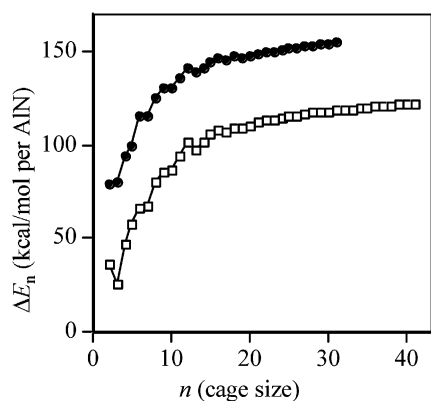


Figure 4. Binding energy ( $\Delta E_n$ , square for HF/LANL2DZ and filled circle for B3LYP/LANL2DZp//LANL2DZ) per AlN unit as a function of the cage size ( $n$ ).

of  $(\text{AlN})_{n+1}$ ,  $(\text{AlN})_{n-1}$ , and  $(\text{AlN})_n$ . Because eq 2 can be considered as disproportionation reaction of a molecule into two fragments, the calculated reaction energy ( $\Delta^2 E_n$ ) can reveal the relative stability of the cluster; that is, a positive value (endothermic) indicates the enhanced stability toward fragmentation, whereas a negative value (exothermic) shows the trend of instability. The same method has been used to estimated the stability of large  $(\text{BH})_n^{2-}$  ( $n = 13-17$ ) cages.<sup>32</sup> As given in Table 2 and shown in Figure 5, the relationship between  $\Delta^2 E_n$  and  $n$  turns out alternatively in increased cages size. It is to

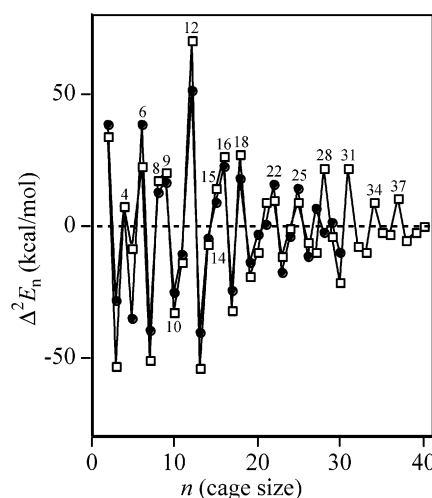


Figure 5. Disproportionation energy ( $\Delta^2 E_n$ , square for HF/LANL2DZ and filled circle for B3LYP/LANL2DZp//LANL2DZ) as a function of the cage size ( $n$ ).

note that HF/LANL2DZ and B3LYP/LANL2DZp//LANL2DZ values have the same trend and pattern:

$$\Delta^2 E_n = (E_{n+1} + E_{n-1})/2 - E_n \quad (2)$$

For  $n < 20$ ,  $(\text{AlN})_n$  clusters with even numbered  $n$  ( $n = 4, 6,$

8, 12, 16, and 18) are more stable than the odd numbered clusters with the exception of  $n = 10$  and 14, as well as 9 and 15 at both HF/LANL2DZ and B3LYP/LANL2DZp/LANL2DZ. In addition to the torsional strain, one factor for this relationship might be the separation of the six  $f_4$  rings, for example, (AlN)<sub>12</sub> has six separated  $f_4$ , whereas (AlN)<sub>11</sub> and (AlN)<sub>13</sub> have only two separated  $f_4$  and two  $f_4$ - $f_4$  annelated rings. The exception for  $n = 10/14$  and  $9/15$  is probably due to the shorter Al–Al distances of the six-membered rings for (AlN)<sub>10</sub> (3.017, 3.108, and 3.170 Å) than for (AlN)<sub>9</sub> (3.066, 3.122, and 3.210 Å). The shortest Al–Al distance of the six-membered rings in (AlN)<sub>14</sub> of 2.956 Å is shorter than that (3.060 Å) in (AlN)<sub>15</sub>. This stability relationship is also found for large (BN)<sub>*n*</sub> cages ( $n = 10$ – $30$ ).<sup>23</sup>

The large disproportionation energy of 51.8 kcal/mol at B3LYP/LANL2DZp/LANL2DZ (70.4 kcal/mol at HF/LANL2DZ) identifies (AlN)<sub>12</sub> as the most stable cluster (the disproportionation energy of (AlN)<sub>12</sub>/ $T_d$  is 52.9 at B3LYP/6-31G\* and 54.7 at B3LYP/6-311G\*\*/B3LYP/6-31G\*, and therefore, the LANL2DZp basis set is reasonable for AlN cages), and this is much larger than those for  $n = 6$  (38.8 vs 22.4 kcal/mol), 8 (12.8 vs 17.1 kcal/mol), 9 (16.5 vs 20.4 kcal/mol), 16 (22.8 vs 26.8 kcal/mol), and 18 (17.9 vs 27.1 kcal/mol). The predicted high stability for (AlN)<sub>12</sub> is supported by the calculated atomization energy.<sup>16</sup> It is interesting to note that (BN)<sub>12</sub> has also been identified as the most stable cage.<sup>23,33</sup> To compare the relative stability, the sheetlike coronene structure and monocyclic ring with alternating Al–N connections for (AlN)<sub>12</sub> have also been computed. This is the same methodology used by Strout for the structure and stability of various (BN)<sub>12</sub> isomers.<sup>33a</sup> It is found that the cage structure of (AlN)<sub>12</sub> is more stable than the sheetlike or monocyclic forms by 246.5 or 405.6 kcal/mol at B3LYP/LANL2DZp (285.4 and 360.4 kcal/mol at HF/LANL2DZ). Therefore, (AlN)<sub>12</sub> should be the ideal candidate for inorganic fullerene-like cage.

## Conclusion

The design and characterization of the most stable (AlN)<sub>*n*</sub> ( $n = 2$ – $41$ ) clusters have been carried out systematically. On the basis of the mathematical relationship for clusters having only four- ( $f_4$ ) and six-membered ( $f_6$ ) rings, the number of  $f_4$  is always equal to 6, whereas the number of  $f_6$  is  $n - 4$ . On this basis and on the fact that cluster with direct N–N and Al–Al connections are less stable, the most stable clusters can be constructed easily using molecular fragments. This qualitative assignment has been confirmed by ab initio and density functional computations. It is found that the  $T_h$  symmetrical (AlN)<sub>12</sub> cluster represents the most stable cage, as indicated by the calculated binding energy per AlN unit and the disproportionation energy.

**Acknowledgment.** This work was supported by the funds of the education ministry of China and by the Youth Science and Technology Foundation of the Shanxi Province, China.

**Supporting Information Available:** Total electronic energies, zero-point energies, and Cartesian coordinates of the most stable cages. This material is available free of charge via the Internet at <http://pubs.acs.org>.

## References and Notes

(1) (a) Ponce, F. A.; Bour, D. P. *Nature (London)* **1997**, *386*, 351. (b) Kiehne, G. T.; Wong, G. K. L.; Ketterson, J. B. *J. Appl. Phys.* **1998**, *84*, 5922. (c) Krupitskaya, R. Y.; Auner, G. W. *J. Appl. Phys.* **1998**, *84*, 2861. (d) Kuo, P. K.; Auner, G. W.; Wu, Z. L. *Thin Solid Films*, **1994**, *253*, 223. (e) Ruiz, E.; Alvarez, S.; Alemany, P. *Phys. Rev. B* **1994**, *49*, 7115. (e)

Wang, X. D.; Jiang, W.; Norton, M. G.; Hipps, K. W. *Thin Solid Films*, **1994**, *251*, 121. (f) Kotula, P. G.; Carter, C. B.; Norton, M. G. *J. Mater. Sci. Lett.* **1994**, *13*, 1275. (g) Rille, E.; Zarwasch, R.; Pulker, H. K. *Thin Solid Films*, **1993**, *228*, 215.

(2) (a) Kim, H. J.; Egashira, Y.; Komiyama, H. *Appl. Phys. Lett.* **1991**, *59*, 2521. (b) Pauleau, Y.; Bouteville, A.; Hantzpergue, J. J.; Remy, J. C.; Cachard, A. *J. Electrochem. Soc.* **1980**, *127*, 1532. (c) Kimura, I.; Hotta, N.; Nukui, H.; Saito, N.; Yasukawa, S. *J. Mater. Sci. Lett.* **1988**, *7*, 66. (d) Kimura, I.; Hotta, N.; Nukui, H.; Saito, N.; Yasukawa, S. *J. Mater. Sci.* **1989**, *24*, 4076.

(3) (a) Egashira, Y.; Kim, H. J.; Komiyama, H. *J. Am. Ceram. Soc.* **1994**, *77*, 2009. (b) Hashman, T. W.; Pratsinis, S. E. *J. Am. Ceram. Soc.* **1992**, *75*, 920. (c) Lee, W. Y.; Lackey, W. J.; Agrawal, P. K. *J. Am. Ceram. Soc.* **1991**, *74*, 1821. (d) Chu, T. L.; Kelm, R. W. *J. Electrochem. Soc.* **1975**, *122*, 995.

(4) (a) Jiang, Z. P.; Interrante, L. V. *Chem. Mater.* **1990**, *2*, 439. (b) Sauls, F. C.; Interrante, L. V. *Coord. Chem. Rev.* **1993**, *128*, 193. (c) Sauls, F.; Interrante, L. V.; Jiang, Z. P. *Inorg. Chem.* **1990**, *29*, 2989. (d) Sauls, F. C.; Hurlley, W. J.; Interrante, L. V.; Marchetti, P. S.; Maciel, G. E. *Chem. Mater.* **1995**, *7*, 1361.

(5) (a) Buc, D.; Hotovy, I.; Hascik, S.; Cerven, I. *Vacuum* **1998**, *50*, 121. (b) Lee, H. C.; Lee, J. Y. *J. Mater. Sci-Mater. El.* **1997**, *18*, 1229. (c) Muhl, S.; Zapien, J. A.; Mendez, J. M.; Andrade, E. *J. Phys. D: Appl. Phys.* **1997**, *30*, 2147.

(6) (a) Watanabe, Y.; Nakamura, Y. *Ceram. Int.* **1998**, *24*, 427. (b) He, X. J.; Yang, S. Z.; Tao, K.; Fan, Y. D. *Mater. Chem. Phys.* **1997**, *51*, 199.

(7) Lester, A.; Zhou, M.; Chertihin, G. V.; Bare, W. D.; Hannachi, Y. *J. Phys. Chem. A* **2000**, *104*, 1656.

(8) Chu, C.; Ong, P. P.; Chen, H. F.; Teo, H. H. *Appl. Surf. Sci.* **1999**, *137*, 91.

(9) (a) Reddy, N. D.; Roesky, H. W.; Noltemeyer, M.; Schmidt, H.-G. *Inorg. Chem.* **2002**, *41*, 2374. (b) Zheng, W.; Roesky, H. W. *J. Chem. Soc., Dalton Trans.* **2002**, 2787.

(10) Lynam, M. M.; Interrante, L. V.; Patterson, C. H.; Messmer, R. P. *Inorg. Chem.* **1991**, *30*, 1918.

(11) Davy, R. D.; Jaffrey, K. J. *J. Phys. Chem.* **1994**, *98*, 8930.

(12) Matsunaga, N.; Gordon, M. S. *J. Am. Chem. Soc.* **1994**, *116*, 11407.

(13) Timoshkin, A. Y.; Bettinger, H. F.; Schaefer, H. F., III. *J. Am. Chem. Soc.* **1997**, *119*, 5668.

(14) Grimes, R. W. *Philos. Mag. B* **1999**, *79*, 407.

(15) <http://webbook.nist.gov/chemistry>.

(16) Chang, C.; Patzer, A. B. C.; Sedlmayr, E.; Steinke, T.; Sulzle, D. *Chem. Phys.* **2001**, *271*, 283.

(17) BelBruno, J. J. *Chem. Phys. Lett.* **1999**, *313*, 795.

(18) Kandalam, A. K.; Blanco, M. A.; Pandey, R. *J. Phys. Chem. B* **2001**, *105*, 6080.

(19) Wu, H.; Xu, X.; Zhang, C.; Zheng, L.; Zhang, Q. *Sci. Chin. Ser. B* **2000**, *43*, 634.

(20) Wu, H.; Zhang, C.; Xu, X.; Zhang, F.; Zhang, Q. *Chin. Sci. Bull.* **2001**, *46*, 1507.

(21) Xu, X.; Wu, H.; Zhang, F.; Zhang, C. *J. Mol. Struct. (THEOCHEM)* **2001**, *542*, 239.

(22) (a) Kandalam, A. K.; Pandey, R.; Blanco, M. A.; Costales, A.; Recio, J. M.; Newsam, J. M. *J. Phys. Chem. B* **2000**, *104*, 4361. (b) Costales, A.; Kandalam, A. K.; Pendas, A. M.; Blanco, M. A.; Recio, J. M.; Pandey, R. *J. Phys. Chem. B* **2000**, *104*, 4368. (c) Nayak, S. K.; Khanna, S. N.; Jena, P. *Phys. Rev. B* **1998**, *57*, 3787. (d) Costales, A.; Blanco, M. A.; Pendas, A. M.; Kandalam, A. K.; Pandey, R. *J. Am. Chem. Soc.* **2002**, *124*, 4116.

(23) Seifert, G.; Fowler, P. W.; Mitchell, D.; Porezag, D.; Frauenheim, T. *Chem. Phys. Lett.* **1997**, *268*, 352.

(24) It is available from [cailiao@sxtu.edu.cn](mailto:cailiao@sxtu.edu.cn).

(25) There are more than 240 possible structures on the basis of the design principle.

(26) Because of the CPU limitation, it was not possible to get the HF/LANL2DZ frequency calculations for  $n > 28$  and the B3LYP/LANL2DZp singlet-point calculations for  $n > 31$ .

(27) Frisch, M. J.; Trucks, G. W.; Schlegel, H. B.; Scuseria, G. E.; Robb, M. A.; Cheeseman, J. R.; Zakrzewski, V. G.; Montgomery, J. A., Jr.; Stratmann, R. E.; Burant, J. C.; Dapprich, S.; Millam, J. M.; Daniels, A. D.; Kudin, K. N.; Strain, M. C.; Farkas, O.; Tomasi, J.; Barone, V.; Cossi, M.; Cammi, R.; Mennucci, B.; Pomelli, C.; Adamo, C.; Clifford, S.; Ochterski, J.; Petersson, G. A.; Ayala, P. Y.; Cui, Q.; Morokuma, K.; Malick, D. K.; Rabuck, A. D.; Raghavachari, K.; Foresman, J. B.; Cioslowski, J.; Ortiz, J. V.; Stefanov, B. B.; Liu, G.; Liashenko, A.; Piskorz, P.; Komaromi, I.; Gomperts, R.; Martin, R. L.; Fox, D. J.; Keith, T.; Al-Laham, M. A.; Peng, C. Y.; Nanayakkara, A.; Gonzalez, C.; Challacombe, M.; Gill, P. M. W.; Johnson, B. G.; Chen, W.; Wong, M. W.; Andres, J. L.; Head-Gordon, M.; Replogle, E. S.; Pople, J. A. *Gaussian 98*; Gaussian, Inc.: Pittsburgh, PA, 1998.

(28) Zurek, E.; Woo, T. K.; Firman, T. K.; Ziegler, T. *Inorg. Chem.* **2001**, *40*, 361.

(29) Coxeter, H. S. M. *Introduction to Geometry*; Wiley: New York, 1961. See also Cerari, M.; Cucinella, S. *The Chemistry of Inorganic Homo- and Heterocycles*; Haiduc, I., Sowerby, D. B., Ed.; Academic Press, New York, 1987; pp 167–190.

(30) Fowler, P. W. *Chem. Phys. Lett.* **1986**, *131*, 444.

(31) This indicates that method rather than the further improvement of basis set is critical for the relative energies.

(32) Schleyer, P. v. R.; Najafian, K.; Mebel, A. M. *Inorg. Chem.* **1998**, *37*, 6765. See also Schleyer, P. v. R.; Najafian, K. *Inorg. Chem.* **1998**, *37*, 3454.

(33) (a) Strout, D. L. *J. Phys. Chem. A* **2000**, *104*, 3364. (b) Strout, D. L. *J. Phys. Chem. A* **2001**, *105*, 261.